Tunneling and percolation transport regimes in segregated composites

B. Nigro, C. Grimaldi, and P. Ryser

Phys. Rev. E **85**, 011137 — Published 20 January 2012

DOI: 10.1103/PhysRevE.85.011137

Tunneling and percolation transport regimes in segregated composites

B. Nigro,[1,*] C. Grimaldi,[1,†] and P. Ryser[1]

[1]*LPM, Ecole Polytechnique Fédérale de Lausanne, Station 17, CP-1015 Lausanne, Switzerland*

We consider the problem of electron transport in segregated conductor-insulator composites in which the conducting particles are connected to all others via tunneling conductances thus forming a global tunneling connected resistor network. Segregation is induced by the presence of large insulating particles which forbid the much smaller conducting fillers to occupy uniformly the three dimensional volume of the composite. By considering both colloidal-like and granular-like dispersions of the conducting phase, modeled respectively by dispersions in the continuum and in the lattice, we evaluate by Monte Carlo simulations the effect of segregation on the composite conductivity σ, and show that an effective medium theory applied to the tunneling network reproduces accurately the Monte Carlo results. The theory clarifies that the main effect of segregation in the continuum is that of reducing the mean inter-particle distances, leading to a strong enhancement of the conductivity. In the lattice segregation case the conductivity enhancement is instead given by the lowering of the percolation thresholds for first and beyond-first nearest neighbors. Our results generalize to segregated composites the tunneling-based description of both the percolation and hopping regimes introduced previously for homogeneous disordered systems.

PACS numbers: 64.60.ah, 73.40.Gk, 72.80.Tm, 72.20.Fr

I. INTRODUCTION

Transport properties of conductor-insulator composites are strongly influenced by the microstructural characteristics of the composite itself. In particular, the dc conductivity σ depends on the volume fraction ϕ of the conducting constituents, on their size [1] and shape [2] as well as on their spatial arrangement in the composite [3, 4]. All those aspects influence σ through their effects on the electrical connectivity of the conductive phase, and can thus be exploited to meet specific criteria for the transport properties in composites.

In compacted mixtures of micrometric conducting and insulating powders [5–8] the electrical connectivity is established by direct contact connections between the conducting particles [4]. In this situation, σ displays an insulator-conductor transition when the concentration ϕ of the conducting phase is such that a macroscopic cluster of connected particles spans the entire sample, allowing the charge carriers to flow between the electrodes. Percolation theory [9, 10] describes such transition by mapping the inter-particle electrical connections to a random resistor network, where the elemental conductances g are either 0 when there is no contact or $g \neq 0$ when two conducting particles touch each other. In this way, percolation theory predicts a power-law behavior of the form $\sigma \simeq (\phi - \phi_c)^t$ for $\phi \gtrsim \phi_c$, where ϕ_c is the critical volume fraction beyond which a spanning cluster is formed and t is a universal transport exponent taking the value $t \simeq 2$ for all three-dimensional systems [10]. For this kind of composites, σ is thus mainly controlled by the value of ϕ_c, which depends upon the shape and the dispersion of the conducting particles.

In nanocomposites made of colloidal dispersions of nanometric conducting particles in an insulating continuous matrix the predominant mechanism of transport is not by direct contact, but rather through indirect electrical connections between particles established by quantum tunneling [11]. For temperatures sufficiently high to neglect particle charging effects, energetic disorder, and Coulomb interaction, the inter-particle conductance decays exponentially for distances between particles larger than a characteristic tunneling length ξ, which measures the electron wave function decay within the insulating phase. Although ξ depends on specific material properties, its value is nevertheless limited to a few nanometers or less, which is a relevant length scale for composites with nanometric conducting particles, whose typical sizes range from tens up to hundreds of nanometers. Hence, besides the effect of shape and dispersion of the conducting constituents, the composite conductivity σ is in this case affected also by the mean distance between the particles, which essentially depends on ϕ.

It is clear that tunneling conduction, albeit decaying fast, does not imply a sharp cutoff of the connectivity between particles and the introduction of a contact-like connectivity criterion, as done for powder mixtures, is not suitable [12]. Conversely, inter-particle conductance by contact can be seen as a limiting case of tunneling when the particle sizes D are much larger than the tunneling decay length ξ, as it is the case for mixtures of micrometric conducting and insulating powders [6–8]. It turns out that it is indeed possible to describe both contact and distance dependent connectivity mechanisms within a single formalism, in which the conducting particles are all electrically connected to each other by tunneling [13]. By using this global tunneling network (GTN) approach, percolation properties of compacted powders or of other granular materials with micrometric conduct-

*Electronic address: biagio.nigro@epfl.ch
†Electronic address: claudio.grimaldi@epfl.ch

ing grain sizes can then be recovered by the $D/\xi \gg 1$ limit of the theory, while hopping transport of colloidal nanocomposites is obtained by much smaller D/ξ values.

As noticed in Ref. [13], D/ξ is not, however, the only factor discriminating between percolation and hopping regimes. Indeed, for D/ξ sufficiently large, the composite microstructure plays the most relevant role and, through the arrangement of the conducting matter in the composite, promotes one regime or the other. For example, homogeneous dispersions of impenetrable conducting spheres in the (insulating) continuum are always characterized by an hopping (or, equivalently, tunneling) type of transport. In this case indeed the conductivity decreases fast but continuously as ϕ is reduced because, in average, the inter-sphere distances increase. Instead, percolation-like behavior of transport arises in close-packed mixtures of conducting and insulating spheres because contact or near-contact clusters of conducting spheres span the entire system for all volume fractions larger than ϕ_c. For large D/ξ, multiple percolation thresholds due to clusters of further next-nearest neighbors can arise in fractionally occupied periodic lattices.

In this article we extend the study of the percolation and hopping regimes to the case of (locally) non-homogeneous dispersions of conducting particles by considering segregation of the conducting fillers due to large (compared to the conducting particles size) insulating inclusions [14–17]. This type of microstructure is rather common in real composites and is at the origin of the large conductivity values measured also for very low contents of the conducting phase. We shall show how this peculiar behavior arises in both hopping and percolating regimes by solving numerically the tunneling network equations for continuum and lattice segregated particle distributions. Furthermore, by using a generalization [13, 18] of the classical effective medium approximation (EMA) [10, 19, 20], we explicitly relate the microstructure properties of the composites with the transport behavior, and provide an approximate but accurate analytic treatment of the conductivity problem, thus extending our previous results for the continuum [17] and generalizing the formulation to the segregated case.

In Sec. II we consider the continuum regime by describing the model for the segregated composites and by introducing the EMA formulation for the calculation of the overall conductance. In Subsec. II A we present the results of both EMA calculation and MC simulations for some segregated systems and in Subsec. II B we provide an explicit approximate analytical formula for the composite conductivity based on EMA. Section. III is devoted to the calculation of both EMA and MC for lattice segregated dispersions of conducting fillers. Finally, Sec. IV is devoted to the conclusions.

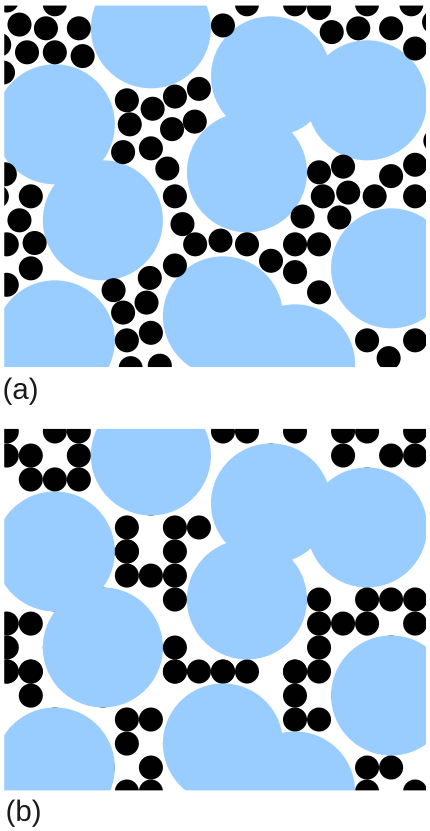

FIG. 1: (Color online) Schematic two-dimensional representation of the segregated dispersions in the continuum (a) and in the lattice (b). The small black circles denote the conducting spheres of diameter D_1 while the larger penetrable circles are the insulating spherical inclusions of diameter D_2. In (b) the centers of the conducting spheres occupy a fraction of the site of a periodic lattice.

II. SEGREGATION IN THE CONTINUUM

Segregation is very common in composite materials such as RuO_2-based cermets [21] or polymer-based composites [22]. This effect is particularly evident when the mean size of the insulating grains (glass-particles or polymeric inclusions as large as few micrometers) is much larger than that of the conducting fillers, whose typical size ranges from tens to hundreds of nanometers. The presence of such large insulating inclusions reduces the volume available for the conducting fillers, which are confined in the remaining space, leading thus to a locally non-homogeneous distribution of the conducting phase in the composite.

In the following we represent the conducting phase of a conductor-insulator composite by generating dispersions of N_1 hard-sphere particles of diameter D_1 and volume fraction $\phi_1 = \rho_1 v_1$, where $v_1 = \pi D_1^3/6$ is the volume of a single sphere, $\rho_1 = N_1/V$ is the number density, and V is

the total volume. The non-segregated (or homogeneous case) is obtained through a random sequential addition (RSA) of hard spheres into a cubic box of side L, followed by an equilibration Monte Carlo (MC) process as described in Ref. [17]. When the RSA limit $\phi_1^{\max} \sim 0.38$ is reached[23], the equilibrium configuration is obtained by placing initially the hard spheres into a cubic lattice and then by relaxing the system through MC runs.

The segregated regime is schematically shown in Fig. 1(a) and is composed by a mixed system of mutually impenetrable conducting and insulating spherical particles. This is obtained by considering a random dispersion of N_2 fully penetrable spheres of diameter D_2 representing the insulating inclusions [16, 17]. We fix the diameter ratio of the two particle species at $D_2/D_1 = 8$, having noticed [17] that this condition is sufficient to characterize segregated systems in the $D_2 \gg D_1$ regime. In addition, in order to minimize size effects, L is chosen as to be at least one order of magnitude larger than D_2. Since the insulating inclusions are placed randomly and are penetrable, the occupied volume fraction is $\phi_2 = 1 - \exp(-v_2\rho_2)$ [24], where $v_2 = \pi D_2^3/6$ and $\rho_2 = N_2/L^3$.

After having placed the insulating spheres, the remaining available space is filled with given densities ρ_1 of conducting hard spheres by means of the same placement and equilibration procedures as for the homogeneous case. Given the mutual impenetrability of the two kinds of spheres, the available volume fraction for arranging the centers of the conducting fillers is given by $v^* = \exp(-V_{\rm ex}\rho_2)$, where $V_{\rm ex} = \pi(D_1 + D_2)^3/6$ is the excluded volume of an insulating sphere with respect to a conducting one. By exploiting the previous definition of ϕ_2, v^* thus reduces to [16]:

$$v^* = (1 - \phi_2)^{(1+D_1/D_2)^3}, \tag{1}$$

which defines an effective filler volume fraction $\phi_{\rm eff} = \phi_1/v^*$.

As stated in the introduction, we consider all conducting particles as electrically connected to all others through tunneling conductances which, for two generic impenetrable spheres i and j of diameter D_1 placed at positions $\mathbf{r}_i$ and $\mathbf{r}_j$, is given by:

$$g_{ij} = g_0 \exp\left(-\frac{2(r_{ij} - D_1)}{\xi}\right), \tag{2}$$

where g_0 is a constant "contact" conductance which will be set equal to the unity in the following, ξ is the characteristic tunneling decay length, and $r_{ij} = |\mathbf{r}_i - \mathbf{r}_j|$ is the distance between two conducting sphere centers.

Contrary to classical resistor networks with few connected nearest neighbors [19], the ensemble of all tunneling conductances forms a fully connected weighted network of N_1 nodes, each having $N_1 - 1$ neighbors. The overall conductivity depends on D_1 and ξ, as well as on the volume fraction ϕ_1 of the particular conducting sphere distribution. Note that the aforementioned mapping between the sphere system and the resistor network holds for both the homogeneous and segregated dispersions of the conducting fillers since the information about the specific distribution is implicit in the weighted links [*i.e.*, the conductances g_{ij} of Eq. (2)] over all sphere centers.

A. EMA and MC

All these dependencies, and in particular the relationship between the spatial particle arrangements and the global transport properties, can be made explicit by employing the EMA formulation developed in Refs. [13, 18], which is a generalization to complete tunneling resistor networks of the classical EMA approach [10, 19, 20]. The original tunneling network is thus replaced by an effective one where all bond conductances are equal to $\bar{g}$, whose value is found by requiring that the effective network has the same average resistance as the original. By considering only two-site clusters [18], the following equation for $\bar{g}$ is found:

$$\left\langle \sum_{i\neq j} \frac{g_{ij} - \bar{g}}{g_{ij} + [(N_1 - 1)/2 - 1]\bar{g}} \right\rangle = 0. \tag{3}$$

where $\langle \ldots \rangle$ indicates a configurational average. By introducing the radial distribution function (RDF) $g_2(r)$ of the N_1 conducting hard spheres defined as [25]:

$$\rho g_2(r) = \frac{1}{N_1} \int \frac{d\Omega}{4\pi} \left\langle \sum_{i\neq j} \delta(\mathbf{r} - \mathbf{r}_{ij}) \right\rangle, \tag{4}$$

equation (3) can be recast as follows

$$\int_0^\infty dr \frac{4\pi r^2 \rho_1\, g_2(r)}{g^* \exp[2(r - D_1)/\xi] + 1} = 2, \tag{5}$$

where $g^* \simeq N_1\bar{g}/2$ is the conductance between any two nodes of the effective network. According to Eq. (5), the whole information about the spatial distribution of the conducting particles is contained in $g_2(r)$, which therefore directly governs the behavior of the EMA conductance g^*. To illustrate how the segregation affects g^* through its effects on $g_2(r)$, we plot in Fig. 2 the numerically calculated RDF for $\phi_1 = 0.114$ and for three different values of the volume fraction ϕ_2 of the insulating spherical inclusions. The $\phi_2 = 0$ case corresponds to a homogeneous dispersion of hard spheres in the continuum, and the resulting RDF (circles) is basically featureless for $r > D_1$ (apart for a slight increase near contact) because of the rather low value of ϕ_1 used. For $\phi_2 > 0$ two features emerge. First, the RDF develops an oscillating behavior with a clear peak at $r \simeq 2D_1$ and a second one, visible for $\phi_2 = 0.6$, at $r \simeq 3D_1$. Second, the RDF is enhanced with respect to the homogeneous case for all values of r lower than $r \simeq D_2 = 8D_1$. These characteristics resemble in part those observed in the RDF of the smaller particles in hard-core mixtures [26] and are indications

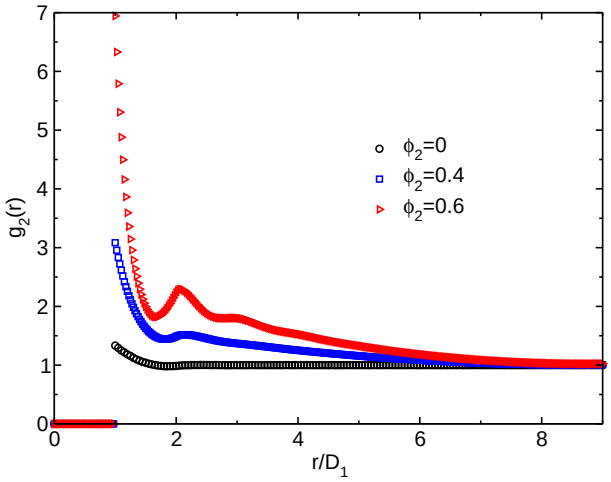

FIG. 2: (Color online) Numerical RDF as a function of the distance in the continuum regime for three different volume fractions of the insulating phase $\phi_2 = 0$, 0.4, and 0.6, for $D_2/D_1 = 8$, and for a fixed filler volume fraction $\phi_1 = 0.114$

of the enhanced probability of having particles separated by a distance $r < D_2$ when $\phi_2 > 0$, which means that the conducting fillers are in average closer to each other when segregation increases. Due to the exponential dependence on the particle separation r_{ij} of the tunneling conductance, Eq. (2), the EMA conductance at fixed ϕ_1 is thus expected to be increased by segregation because, for $\phi_2 > 0$, particles have lower average value of r_{ij}.

This is confirmed by the results plotted in Fig. 3(a), where the EMA conductance g^*, obtained from solving Eq. (5) with $g_2(r)$ evaluated from MC calculations, is reported as a function of ϕ_1 and for $\phi_2 = 0$, 0.4, and 0.6. The role of segregation in enhancing g^* is made even more evident when D_1/ξ increases, as it can be inferred by comparing the results in the upper panel of Fig. 3(a), obtained for $D_1/\xi = 15$, with those with $D_1/\xi = 50$ in the lower panel.

The result that the EMA formulation provides a transparent relation between the microstructure of segregated continuum composites, contained in $g_2(r)$, and the transport behavior is made even more firm by the fact that the EMA conductance is in excellent accord with our fully numerical calculations of σ [27]. These are shown in Fig. 3(b), and have been obtained by the same numerical procedures described in Ref. [17] consisting in solving numerically the Kirchoff equations of the tunneling resistor network with conductances given by Eq. 2. For the segregated cases, each symbol in Fig. 3(b) is the outcome of $N_R = 200$ realizations for N_1 conducting particles ranging from a few hundreds for low ϕ_1 to hundreds of thousands for the higher values, by keeping L fixed. Instead for the homogeneous case ($\phi_2 = 0$) $N_R = 500$ has been considered, with N_1 fixed at $\simeq 1000$.

B. EMA analytical formula

The good agreement between the EMA results and the fully numerical σ in both the homogeneous and segregated regimes suggests that further insights can be gained directly from the EMA equation (5). Hence we proceed here with some further approximations in the attempt to find an analytical expression for the EMA conductance. We start by noticing that the integral in Eq. (5) can be rewritten as

$$\int_0^\infty dr 4\pi r^2 \rho_1 \, g_2(r) W(r) = 2, \tag{6}$$

where

$$W(r) = \frac{1}{\exp\left[\frac{2}{\xi}(r - r^*)\right] + 1}, \tag{7}$$

and r^* is defined by the following relation:

$$g^* = \exp\left[-\frac{2}{\xi}(r^* - D_1)\right]. \tag{8}$$

We note that for large values of D_1/ξ, which is the regime of practical interest for our purposes [17] (see also Sec. I), $W(r)$ is well approximated by $\theta(r^* - r)$, where $\theta(x)$ is 1 for $x \geq 0$ and 0 otherwise. Thus, by adopting the definition of the cumulative coordination number

$$Z(r) = \int_0^r dr' 4\pi r'^2 \rho_1 g_2(r'), \tag{9}$$

which gives the number of spheres whose centers are within a distance r from the center of a given sphere, we obtain the following approximation of Eq. (5):

$$Z(r^*) = 2. \tag{10}$$

Equation (8), where r^* is such that Eq. (10) is satisfied, is plotted in Fig. 3(a) (star symbols) and is in close agreement with the numerical solution of Eq. (5). We proceed further by noticing that the quantity $\delta^* \equiv r^* - D_1$ is the EMA equivalent of the critical distance δ_c found by the critical path approximation (CPA) for the tunneling conductivity [28, 29]. The CPA δ_c, plotted in Fig. 4 (symbols) as a function of ϕ_1 for $\phi_2 = 0$, 0.4 and 0.6, is the shortest among the interparticle distances such that the subnetwork formed by those particles having $r_{ij} - D_1 \leq \delta_c$ forms a percolating cluster. Equivalently, δ_c is such that $Z(\delta_c + D_1) = Z_c$ is satisfied, where Z_c is the critical coordination number which, for the homogeneous case $\phi_2 = 0$, ranges between $Z_c \simeq 2.7$ for $\phi_1 \to 0$ and $Z_c \simeq 1.5$ for $\phi_1 \simeq 0.5$ [30]. It turns out therefore that the right-hand side of Eq. (10) falls well within the range of possible Z_c values, which is the ultimate reason of the good accord between the EMA approximation of the conductance and the fully numerical σ already noticed in Ref. [13] for the homogeneous case.

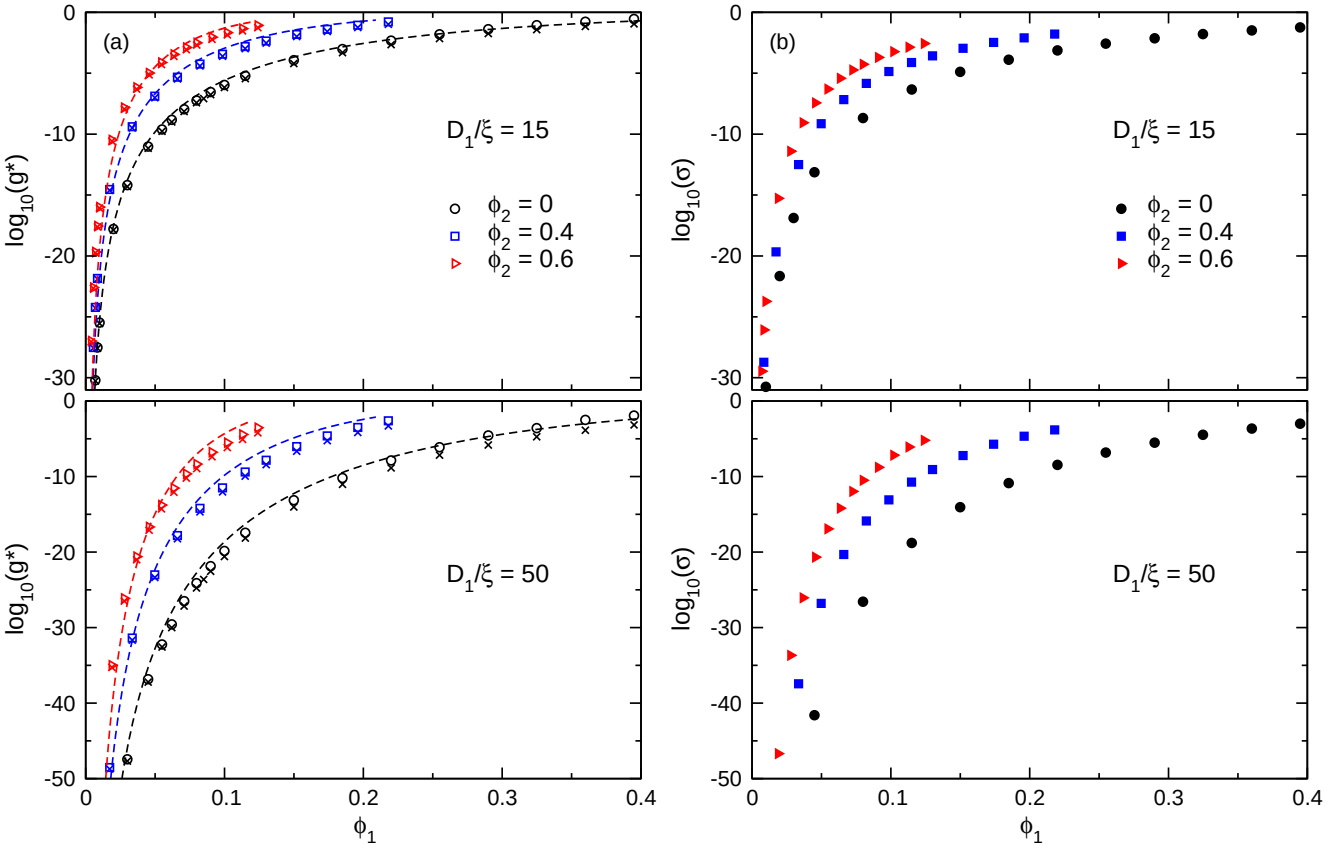

FIG. 3: (Color online) (a) Calculated EMA conductance g^* (open symbols) as a function of the volume fraction ϕ_1 of the conducting spheres of diameter D_1 for $D_1/\xi = 15$ and 50, and for different values of the volume fraction $\phi_2 = 0$, 0.4, and 0.6 of the insulating spheres with diameter D_2 and diameter ratio $D_2/D_1 = 8$. The crosses and the dashed lines refer respectively to Eq. (8), where r^* is such that $Z(r^*) = 2$ is satisfied, and to Eq. (14). (b): conductivity σ for the same parameters as in (a) obtained from the numerical solution of the tunneling resistor equations.

By noticing from Fig. 4 that $\delta^* \ll D_1$ for large ϕ_1 values and that $g_2(r) = 0$ for $r < D_1$, in order to correctly capture the high density regime, we approximate the RDF in Eq. (9) with its contact value $g_2(D_1)$. In this way, Eq. (10) can be rewritten as

$$g_2(D_1) \int_0^{D_1+\delta^*} dr 4\pi r^2 \rho_1 \theta(r - D_1) = 2, \qquad (11)$$

which can be solved for δ^* leading to:

$$\delta^* = r^* - D_1 = D_1 \left[1 + \frac{1}{4\phi_1 g_2(D_1)} \right]^{1/3} - D_1. \qquad (12)$$

By using the Carnahan-Starling formula $g_2(D_1) = (1 - \phi_1/2)/(1 - \phi_1)^3$ for the RDF at contact [31], which is a well-known approximation used in the theory of simple liquids [25], Eq. (12) turns out to be a rather good approximation for δ_c in the whole range of densities for $\phi_2 = 0$ (solid line in Fig. 4), and thus we can use the same approximate scaling relation that we formulated in Ref. [17] for the critical distance δ_c of segregated systems. Hence, if $\delta^*(\phi_1, \upsilon^*)$ is the EMA critical distance for a segregated system parametrized by the available volume υ^* of Eq. (1), then

$$\delta^*(\phi_1, \upsilon^*) = \upsilon^{*-1/3} \delta^*(\phi_{\rm eff}), \qquad (13)$$

where $\phi_{\rm eff} = \phi_1/\upsilon^*$ is the effective volume fraction for the conducting fillers introduced in Sec. II. Equation (13) then states that the EMA critical distance in the segregated regime can be directly obtained from that of the homogeneous case calculated at $\phi_{\rm eff}$. As shown in Fig. 4, Eq. (13) compares well with MC calculations of the critical distance δ_c, so that by using Eq. (8) with Eqs. (12) and (13) and $g_2(D_1)$ as given by the Carnahan-Starling expression we obtain the following approximated analytical formula of the EMA conductance:

$$g^* = \exp\left\{ -\frac{2D_1}{\xi \upsilon^{*\frac{1}{3}}} \left[\left(\frac{1 + \phi_{\rm eff} + \phi_{\rm eff}^2 - \phi_{\rm eff}^3}{2\phi_{\rm eff}(2 - \phi_{\rm eff})} \right)^{\frac{1}{3}} - 1 \right] \right\}. \qquad (14)$$

The above expression is plotted in Fig. 2(a) by dashed lines and turns out to be in very good agreement with the full solution of the EMA integral of Eq. (5). Hence,

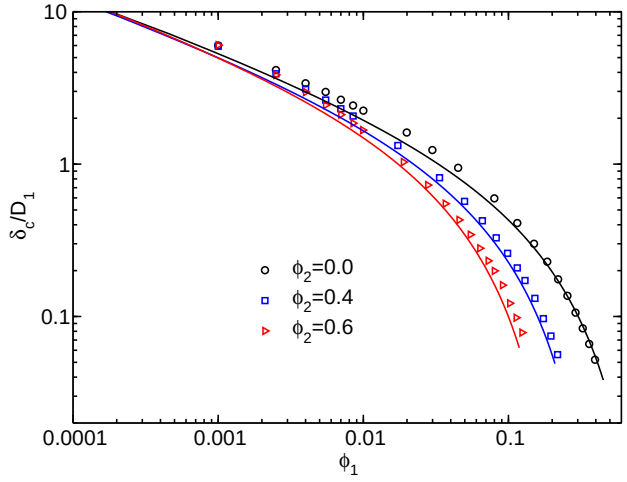

FIG. 4: (Color online) Critical distance δ_c dependence on the volume fraction ϕ_1 of the conducting spheres for $\phi_2 = 0$, 0.4, and 0.6 and for $D2/D1 = 8$ extracted from MC calculations [17]. Solid lines: our δ^* approximation from Eq. (12) ($\phi_2 = 0$) and from Eq. (13) ($\phi_2 \neq 0$).

despite of its simplicity, Eq. (14) effectively captures the conductance behavior of both the homogeneous and segregated cases in the whole range of ϕ_1 values, thus generalizing the results of Refs. [12, 13, 17].

III. SEGREGATION IN THE LATTICE

Segregation can be induced in powder mixtures of conducting and insulating particles when the mean size of the insulating grains is much larger than that of the conducting ones. Typical examples of segregated powder mixtures and of the corresponding conductivity measurements can be found in Refs. [5, 8]. Compared to powder mixtures of conducting and insulating grains with comparable mean sizes [6, 7], the conductivity of segregated powders drops by several orders of magnitude at much lower values of the volume fraction.

In order to describe the effect of segregation in powder mixtures, we consider a model composite where the conducting particles occupy only a fraction p of the total M sites of a simple cubic lattice. For non-segregated systems, we consider equal sized conducting and insulating particles of spherical shape with diameter equal to the lattice spacing, as in the Scher and Zallen model [32]. For a random distribution of the conducting spheres on the cubic lattice the corresponding RDF reduces to [13]:

$$\rho g_2(r) = \frac{p}{4\pi} \sum_{k=1,2,\ldots} \frac{\mathcal{N}_k}{R_k^2}\, \delta(r - R_k), \qquad (15)$$

where $\mathcal{N}_k$ is the number of the kth nearest neighbors being at distance R_k from a reference particle set at the origin. From Eq. (15), and by using the tunneling interparticle conductance of Eq. (2), the EMA equation (5) becomes

$$p \sum_{k=1,2,\ldots} \frac{\mathcal{N}_k}{g^* \exp[2(R_k - D_1)/\xi] + 1} = 2, \qquad (16)$$

whose solution is plotted in Fig. 5(a) (solid black lines) as a function of the volume fraction ϕ_1 of the conducting phase ($\phi_1 = p\pi/6$) for two different values of D_1/ξ. As discussed in more details in Ref. [13], the decrease of g^* as $\phi_1 \to 0$ is characterized by sharp drops at $\phi_1^k = p_k\pi/6$ where $p_k = 2/(\sum_{k'=1}^{k} \mathcal{N}_{k'})$ is the percolation threshold for the kth nearest neighbors. This behavior is due to the discrete nature of the lattice RDF, Eq. (15), and is confirmed by the full MC results shown in Fig. 5(b), where the conductivity is obtained by following the same procedure of the continuum regime for the number of particles held fixed at $N_1 \sim 1000$.

Since in real segregated powder mixtures the conducting particle sizes are in the micro-metric range [5, 8], the corresponding large values of D_1/ξ make the percolation threshold for particles at contact $p_1 = 2/\mathcal{N}_1$ (= 1/3 for a cubic lattice) the one of practical interest. In this regime, and for $\phi_1 \gtrsim \phi_1^1$, the EMA conductance and the Monte Carlo conductivity follow the power-law behaviors $g^* \propto (\phi_1 - \phi_1^1)$ and $\sigma \propto (\phi_1 - \phi_1^1)^t$, with respectively $\phi_1^1 = \pi/18 \simeq 0.174$ and $\phi_1^1 \simeq 0.163$, where $t \simeq 2$ is the transport exponent for three-dimensional systems [13].

In analogy with the continuum segregation of Sec. II, we consider the segregation in the lattice as being due to N_2 penetrable and insulating spheres of diameter D_2 placed at random in the cubic volume. As schematically shown in Fig. 1(b), the conducting particles will thus occupy randomly only those lattice sites lying outside the insulating spheres and not leading to overlaps between the two species of particles. As for the homogeneous random lattice case, the RDF of the segregated lattice is given by a series of delta-peaks centered at R_k, as in Eq. (15), but with the number $\mathcal{N}_k$ of the kth nearest neighbors being dependent of D_2/D_1 and of the volume fraction ϕ_2 of the insulating spheres. In Fig. 6 we show the R_k dependence of $\mathcal{N}_k(\phi_2)$ in units of the number of the kth nearest neighbors for the homogeneous lattice $\mathcal{N}_k(0)$ for $D_2/D_1 = 8$ and for $\phi_2 = 0.4$ and 0.6. For $R_k \gg D_1$ the ratio $\mathcal{N}_k(\phi_2)/\mathcal{N}_k(0)$ approaches unity which indicates that at large distances segregation plays a minor role, a result similar to the one found for the continuum segregation case (see Fig. 2). On the contrary, for R_k values close to contact, segregation enhances the number of kth nearest neighbors for fixed ϕ_1 because, again in analogy with the continuum case, the reduced available volume enhances the probability of finding conducting particles at distances lower than about D_2. By presuming that the enhanced local probability can be approximated by $p_1^* = p_1/\upsilon^*$, then $\mathcal{N}_k(\phi_2)/\mathcal{N}_k(0)$ should scale as $1/\upsilon^*$ for R_k sufficiently close to contact (and D_2/D_1 sufficiently large), which is a fair approximation for $\phi_2 = 0.4$ but a less satisfactory one for $\phi_2 = 0.6$ (horizontal dashed lines in Fig. 6).

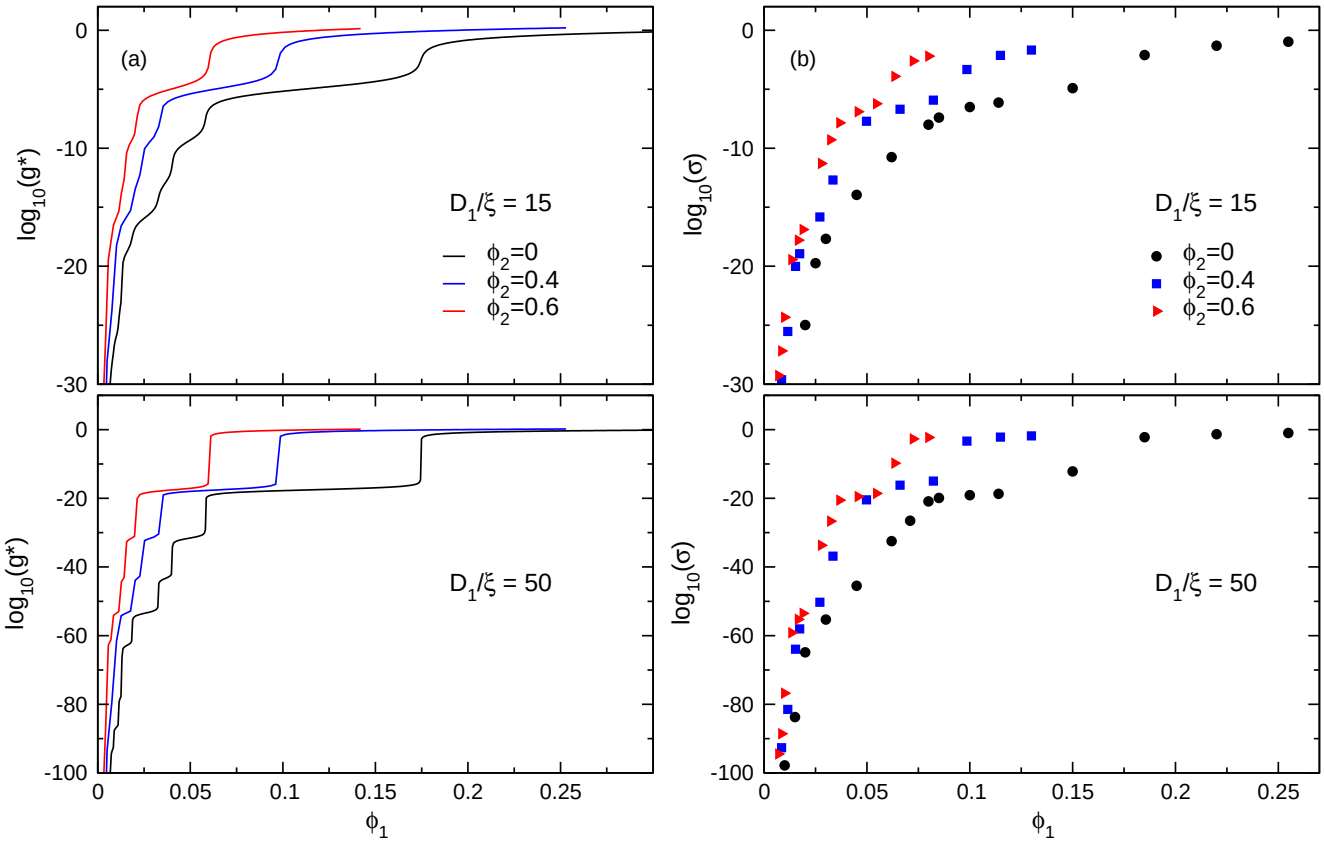

FIG. 5: (Color online) (a) Calculated EMA conductance g^* for the segregated lattice as a function of the volume fraction ϕ_1 of the conducting spheres for $D_1/\xi = 15$ and 50, and for different values of the volume fraction ϕ_2 of the insulating spheres with diameter D_2. (b): conductivity σ for the same parameters as in (a) obtained from the numerical solution of the tunneling resistor equations.

From $p_k(\phi_2) = 2/[\sum_{k'=1}^{k} \mathcal{N}_{k'}(\phi_2)]$ and $\mathcal{N}_k(\phi_2) > \mathcal{N}_k(0)$ it follows immediately that the percolation thresholds $p_k(\phi_2)$ for the kth nearest neighbors in the segregated lattice are lower than those for the homogeneously random lattice $p_k(0)$. In particular, the percolation threshold of particles at contact is reduced by the factor $\mathcal{N}_1(0)/\mathcal{N}_1(\phi_2)$ which from Fig. 6 is 0.54 and 0.33 for $\phi_2 = 0.4$ and $\phi_2 = 0.6$, respectively. Note that approximating $p_1^1(\phi_2)/p_1^1(0)$ with υ^* leads to 0.48 for $\phi_2 = 0.4$ and to 0.27 for $\phi_2 = 0.6$.

The systematic lowering of $p_k(\phi_2)$ as ϕ_2 is enhanced is reflected in the ϕ_1-dependence of the EMA conductance g^* in Fig. 5(a) obtained by solving numerically Eq. (16) with our calculated values of $\mathcal{N}_k(\phi_2)$. The overall effect of segregation is thus the enhancement of g^* with respect to the homogeneous lattice case at $\phi_2 = 0$ induced by the downshift of all $p_k(\phi_2)$ values. This behavior is confirmed by the full MC results of Fig. 5(b), which have been obtained by solving the tunneling resistor network for N_1 ranging from a few hundreds for $\phi_1 \sim 10^{-3}$ to $N_1 \sim 230000$ for $\phi_1/\upsilon^* \sim 0.5$ with L held fixed at $L = 10D_2$. Given the above results and discussion, the conductivity for segregated micrometric (i.e., $D_1/\xi \gg 1$) powders just above the percolation threshold is expected thus to follow approximately $\sigma \propto (\phi_1 - \phi_1^1\upsilon^*)^t$ where ϕ_1^1 is the critical volume fraction for conducting particles at contact in the absence of segregation. Due to the quasi-invariance of ϕ_1^1, according to which $\phi_1^1 \approx 0.17$ independently of the (three dimensional) lattice topology [32], this result is expected to apply also to non-cubic segregated lattices.

IV. CONCLUSIONS

In this paper we have considered the dc electrical transport problem in two-phase segregated amorphous solids, where large insulating inclusions prevent the smaller conducting particles to be dispersed homogeneously in the three dimensional volume. By taking into account explicitly the tunneling mechanism of electron transfer between conducting particles, we have studied the effect of segregation for both continuum and lattice models of composites. For continuum segregated composite materials, we have shown by theory and Monte Carlo simulations that segregation basically reduces the inter-particle

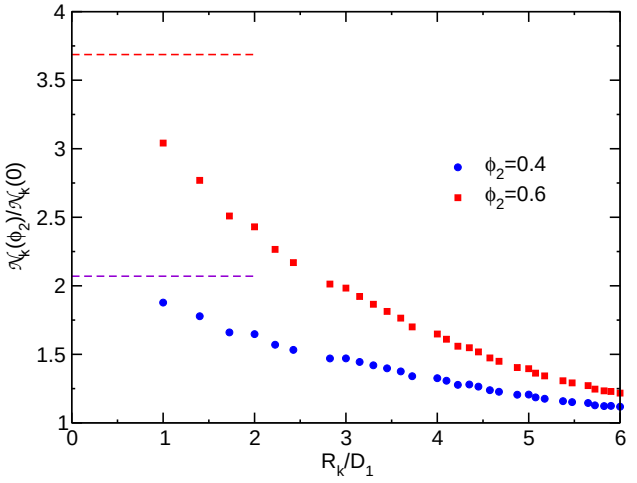

FIG. 6: (Color online) Enhancement ratio of the number $\mathcal{N}_k$ of kth neighbors for $\phi_2 = 0.4$ and 0.6 (for $D_2/D_1 = 8$) as compared to the non-segregated case $\phi_2 = 0$. R_k is the distance of the kth neighbor lattice site from a reference site. The dashed lines are $1/v^*$

distances leading to a strong enhancement of the overall tunneling conductivity. In particular we have evidence how this enhancement can be quasi-quantitatively reproduced by using an effective medium theory applied to the tunneling resistor network, according to which the effect of segregation on the composite microstructure is contained entirely in the radial distribution function for the conducting particles. By using some simple geometrical considerations in combination with the effective medium approximation we have been able to provide an explicit formula for the composite conductivity as a function of the conducting filler content and of the degree of segregation. When applied to our model of lattice segregation, we have demonstrated how the effective medium theory closely reproduces the Monte Carlo results for the conductivity, which can be interpreted as due to a reduction of the available lattice sites for placing the conducting particles.

Acknowledgments

This work was supported by the Swiss National Science Foundation (Grant No. 200021-121740).

[1] X. Jing, W. Zhao, and L. Lan, J. Mater. Sci. Lett. **19**, 377 (2000).

[2] T. Ota, M. Fukushima, Y. Ishigure, H. Unuma, M. Takahashi, Y. Hikichi, and H. Suzuki, J. Mater. Sci. Lett. **16**, 1182 (1997); K. Nagata, H. Iwabuki, and H. Nigo, Compos. Interfaces **6** 483 (1999).

[3] C. -W. Nan, Y. Shen, and J. Ma, Annu. Rev. Mater. Res. **40**, 131 (2010).

[4] D. S. McLachlan and G. Sauti, J. Nanomater. **2007**, 30389 (2007)

[5] A. Malliaris and D. T Turner, J. Appl. Phys. **42**, 614 (1971).

[6] J. Wu and D. S. McLachlan, Phys. Rev. B **56**, 1236 (1997).

[7] E. Thommerel, J. C. Valmalette, J. Musso, S. Villain, J. R. Gavarri, and D. Spada, Materials Science and Engineering A 328, 67 (2002).

[8] C. Chiteme and D. S. McLachlan, Phys. Rev. B **67**, 024206 (2003).

[9] D. Stauffer and A. Aharony, *Introduction to Percolation Theory* (Taylor & Francis, London 1994).

[10] M. Sahimi, *Heterogeneous Materials I. Linear Transport and Optical Properties* (Springer, New York, 2003).

[11] I. Balberg, J. Phys. D: Appl. Phys. **42**, 064003 (2009).

[12] G. Ambrosetti, C. Grimaldi, I. Balberg, T. Maeder, A. Danani, and P. Ryser, Phys. Rev. B **81** , 155434 (2010).

[13] G. Ambrosetti, I. Balberg, and C. Grimaldi, Phys. Rev. B **82**, 134201 (2010).

[14] R. P. Kusy, J. Appl. Phys. **48**, 5301 (1977).

[15] D. He and N. N. Ekere, J. Phys. D: Appl. Phys. **37**, 1848 (2004).

[16] N. Johner, C. Grimaldi, T. Maeder, and P. Ryser, Phys. Rev. E **79**, 020104(R) (2009).

[17] B. Nigro, G. Ambrosetti, C. Grimaldi, T. Maeder, and P. Ryser, Phys. Rev. B **83**, 064203 (2011).

[18] C. Grimaldi, EPL Europhys. Lett. **96**, 36004 (2011).

[19] S. Kirkpatrick, Rev. Mod. Phys. **45**, 574 (1973).

[20] D. A. G. Bruggeman, Ann. Phys. **24**, 636 (1935); R. Juretschke, R. Landauer, and J. A. Swanson, J. Appl. Phys. **27**, 838 (1956);

[21] G. E. Pike and C. H. Seager, J. Appl. Phys. **48**, 5152 (1977); P. F. Carcia, A. Ferretti, and A. Suna, J. Appl. Phys. **53**, 5282 (1982); A. Kusy, Physica B **240**, 226 (1997); A. Alessandrini, G. Valdrè, B. Morten, and M. Prudenziati, J. Appl. Phys. **92**, 4705 (2002)

[22] J. C. Grunlan, W. W. Gerberich, and L. F. Francis, J. Appl. Polym. Sci., **80**, 692 (2001); Polym. Eng. Sci., **41** 1947 (2001); Y.P. Mamunya, V. V. Davydenko, P. Pissis, and E. V. Lebedev, Eur. Polym. J. **38** 1887 (2002).

[23] J. D. Sherwood, J. Phys. A **30**, L839 (1997).

[24] S. Torquato, *Random Heterogeneous Materials: Microstructure and Macroscopic Properties* (Springer, New York, 2002).

[25] J. -P. Hansen and I. R. McDonald, *Theory of Simple Liquids* (Elsevier, London, 2006).

[26] Y.-X. Yu and J. Wu, J. Chem. Phys. **117**, 10156 (2002).

[27] It should be kept in mind that g^* is a two-point conductance raher than a conductivity. For a complete network of identical resistors, as it is the EMA effective network, g^* is indeed the meaningful quantity for describing transport.

[28] V. Ambegaokar, B. I. Halperin, and J. S. Langer, Phys. Rev. B **4**, 2612 (1971); M. Pollak, J. Non Cryst. Solids **11**, 1 (1972); B. I. Shklovskii and A. L. Efros, Sov. Phys.

JETP **33**, 468 (1971); **34**, 435 (1972); C. H. Seager and G. E. Pike, Phys. Rev. B **10**, 1435 (1974).
[29] Y. M. Strelniker, S. Havlin, R. Berkovits, and A. Frydman, Phys. Rev. E **72**, 016121 (2005)
[30] D. M. Heyes, M. Cass, and A. C. Brańca, Mol. Phys. **104**, 3137 (2006).
[31] N. F. Carnahan and K. E. Starling, J. Chem. Phys. **51**, 635 (1969).
[32] H. Scher and R. Zallen, J. Chem. Phys. **53** 3759 (1970).